

Physical behavior of the mixed chain diacylglycerol, 1-stearoyl-2-oleoyl-*sn*-glycerol: difficulties in chain packing produce marked polymorphism

Li Di and Donald M. Small¹

Department of Biophysics, Housman Medical Research Center, Boston University School of Medicine, 80 East Concord Street, Boston, MA 02118-2394

Abstract Diacylglycerols (DAG) play an important role in metabolism, signal transduction and protein kinase activation. Naturally occurring DAGs usually contain a saturated chain in the 1-position and an unsaturated chain in the 2-position. We have investigated the physical behavior of 1-stearoyl-2-oleoyl-*sn*-glycerol (*sn*-SODG) both in the dry and hydrated states by means of differential scanning calorimetry, X-ray diffraction, and NMR. In the dry state the saturated stearate and unsaturated oleate chains have difficulties in packing. As a result marked polymorphism occurs as the chains try to find a suitable packing. Eight phases were found in the dry state: α (transition temperature = 16.4°C; ΔH = 6.8 kcal/mol); β_4 , (20.7°C; 13.8); β_3 (21.5°C; 13.8); β_2 (22.2°C; 14.4); β_1 (23.1°C; 12.3); β' (25.7°C; 11.9); γ_1 (-2.9°C; 0.5), and γ_2 (-5.9°C; 1.2), all of relatively low stability compared to 1,2 distearoyl-*sn*-glycerol (β' , 77.2°C; 30.6). γ_1 and γ_2 are metastable low temperature phases. β_1 - β_4 are bilayers (d_{001} = 34.5, 43.4, 44.7, 46.1 Å, respectively) with elements of triclinic parallel chain packing, while β' is a bilayer (d_{001} = 47.1 Å) with orthorhombic perpendicular chain packing. The metastable α phase has hexagonal chain packing and an unusual eight-layer structure (d_{001} = 174 Å). Hydrated *sn*-SODG contains about one-half of a water molecule per diacylglycerol. Three phases can be distinguished γ_w , α_w (15.1°C; 6.7) and β_w (19.9°C, 14.3). Both α_w and β_w are bilayers but α_w has hexagonal chain packing and β_w is predominantly triclinic parallel packing. Thus, when saturated and unsaturated chains must pack side by side, complex chain conformation, disorder, and instability result giving rise to marked polymorphism. Hydration appears to partly stabilize the interactions. — **Di, L., and D. M. Small.** Physical behavior of the mixed chain diacylglycerol, 1-stearoyl-2-oleoyl-*sn*-glycerol: difficulties in chain packing produce marked polymorphism. *J. Lipid Res.* 1993. **34**: 1611-1623.

Supplementary key words differential scanning calorimetry • nuclear magnetic resonance • X-ray diffraction • membrane bilayers

Diacylglycerols (DAG) are central molecules in the metabolism of fats and phospholipids (1). Generally, DAG are minor lipid constituents in the membranes of cells but they play key roles in a variety of biological processes.

The biologically active isomer is 1,2-diacyl-*sn*-glycerol (1,2-DAG). They are the final substrate in the formation of the major storage lipid, triacylglycerol. The enzyme diacylglycerol acyltransferase esterifies an activated fatty acid to the 3-position of 1,2-diacyl-*sn*-glycerol to form triacylglycerol. 1,2-Diacylglycerol can be phosphorylated to phosphatidic acid by DAG kinase. Phosphatidic acid is a precursor of a number of important phospholipids such as phosphatidylserine, phosphatidylinositol, and phosphatidylglycerol. Phosphatidylethanolamine and phosphatidylcholine can be directly formed from 1,2-diacylglycerol through transfer of phosphoethanolamine or phosphocholine from CDP-ethanolamine and CDP-choline to 1,2-DAG by transferases. DAG is also a substrate for diglyceride lipase which cleaves an acid leaving monoacylglycerol. The fatty acid cleaved may be arachidonic acid or another polyunsaturated fatty acid that are precursors of prostaglandins and leukotrienes. DAG are also intermediate products of lipolysis reactions (2). Intestinal lipases (gastric or lingual, pancreatic, carboxy-ester lipases) hydrolyze the fatty acids from the primary glycerol carbons (1 and 3) to produce first DAGs and finally 2 moles of fatty acid and 1 mole of 2-monoacylglycerol. Lipoprotein lipase and hepatic triglyceride lipase also catalyze the hydrolysis of plasma triglycerides to diacyl and monoacyl glycerides. Finally the role of DAG in the phosphatidylinositol cycle is well known (3-5). The DAG formed in that reaction acts as an activator of protein kinase C and thus becomes an important molecule in regulating transduction of intracellular signals across the plasma membrane. Only the 1,2-diacyl-*sn*-glycerol isomer is able to activate protein kinase C (6, 7).

The physical properties of a few 1,2-diacyl-*sn*-glycerols

Abbreviations: DAG, diacylglycerol; *sn*-SODG, 1-stearoyl-2-oleoyl-*sn*-glycerol; DSC, differential scanning calorimetry; NMR, nuclear magnetic resonance; TLC, thin-layer chromatography.

¹To whom correspondence should be addressed.

have been reported. However, most of the studies describe saturated chain diacylglycerols. For instance, the crystal structure of the β' form of 1,2-dilauroyl-*sn*-glycerol was reported by Pascher, Sundell, and Hauser (8). Dorset and Pangborn (9) reported a single crystal structure of the β' form of 1,2-dipalmitoyl-*sn*-glycerol that was isostructural with the structure reported for dilauroyl-*sn*-glycerol molecule (8). Recently, we have reported on the structure and polymorphism of a series of saturated monoacid 1,2-diacyl-*sn*-glycerols synthesized from fatty acids with 12–24 carbons, (10). The phase behavior of these stereospecific diacylglycerols is relatively straightforward. The shorter chain molecules ranging from C12 to C18 have a stable bilayered β' phase, isostructural with the Pascher et al. (8) and Dorset and Pangborn (9) structures, which melt at increasing temperature the longer the chain (C12 = 47.5°C, C16 = 70.1°C, C18 = 77.2°C). On cooling several degrees below the β' melting point, a metastable bilayered α phase with hexagonally packed chains is formed. With incubation at temperatures below the α melting point, the α phase will convert to the β' phase with time. The behavior patterns of the long chain C22 and C24 1,2-diacyl-*sn*-glycerols are similar, except that on cooling of the α phase, a sub- α phase is formed with pseudo-hexagonal chain packing. All of the structures are bilayered and consist of orthorhombic perpendicular chain packing or a form of hexagonal chain packing. We have also studied the behavior of 1,2-dilauroyl diglyceride (DLG) in phospholipid bilayers and found the glycerol conformation to be different from that in the crystalline β' form (11). In fact, it is quite similar to that of a phospholipid in a bilayer, in that the glycerol backbone is perpendicular to the plane of the bilayer with the hydroxyl group extended out of the bilayer and hydrogen bonded to water. Like phosphatidylcholine (12), the *sn*-2 chain bends over at the second carbon to lie parallel to the *sn*-1 chain. Using ^{13}C -labeled DLG we were able to estimate the transbilayer diffusion (flip flop) of DLG across the phospholipid bilayer. A rate constant at 38°C of about 60 s⁻¹ was found (11).

Most biologic diglycerides, however, do not contain just saturated chains but most often have a saturated chain in the 1-position and an unsaturated chain in the 2-position. However, saturated chains do not mix well with unsaturated chains (13). It is striking to note that when octadecane is mixed with 9-*cis*-octadecene no mixing in the solid state occurs (14). No eutectics, solid solutions, or compounds are formed. Thus, the question of how chain packing would be accommodated in a molecule with both types of chain attached to the glycerol is an interesting problem. A number of conformations have been suggested, some by computer modeling and others by analogy to other molecules having dissimilar chains. A possible packing was suggested that involves the lateral segregation of rows of unsaturated chains from rows of

saturated ones within the plane of the monolayer (14). Using computer modeling, Applegate and Glomset (15–17) calculated conformations for 1-stearoyl-2-oleoyl glycerol chain packing. They assumed that the glycerol-carbonyl region of the molecule had the crystalline conformation of phosphatidylethanolamine (18) and a *trans-antiskew-cis-antiskew-antigauche-trans* conformation around the C-C-C=C-C-C-C which forces the two dissimilar chains to pack side by side. In many conformations the packing energy was unfavorable (15–17). The most favored conformation in monolayers (17) allowed maximal interaction of oleate chains in adjacent rows of molecules to form linear domains of 18:1 separated from linear domains of 18:0 chains in the monolayer, rather like that suggested earlier (14).

If the chains in the 1 position can point in the opposite direction from those in the 2 position to form an extended conformation like 1,3 diacylglycerols (19), then the saturated chains can form one layer and the unsaturated chains a separate layer. This kind of chain segregation occurs in several mixed chain triacylglycerols and can result in trilayer or hexalayered structures (13, 20–22). Given the paucity of information, it seemed important to study mixed chain DAGs in which a saturated 18 carbon chain was present on the 1-position and an unsaturated 18 carbon chain on the 2-position. Thus our group (23) has synthesized 1-stearoyl-2-oleoyl-*sn*-glycerol (*sn*-SODG) and we have studied its physical behavior and polymorphism in the dry state and in the presence of water by X-ray diffraction, differential scanning calorimetry (DSC), and NMR. It is evident from the large number of polymorphic forms of rather similar energy formed that the two chains have difficulty in deciding what is the most favorable conformation.

MATERIALS AND METHODS

Synthesis

sn-SODG were synthesized as described by Kodali and Duclos (23). The purities of the compounds were checked by thin-layer chromatography (TLC) and ^1H NMR and were found to be >99% pure. The occurrence of polymorphism was examined with two kinds of samples: crystallized from melt and crystallized from solvent. The samples crystallized from solvent were made by crystallizing the compounds from hexane in a cold room (4°C) through slow evaporation. The crystalline samples were kept at low temperatures (0–4°C) during packing into X-ray and DSC containers to avoid melting. The 1,2-diglycerols were handled with care during the experiments to avoid 1,3-acyl migration (24). At the end of selected DSC and X-ray experiments, the sample was removed and checked for hydrolysis and acyl migration by TLC (24).

DSC experiments

Dry *sn*-SODG DSC was carried out on a Perkin-Elmer DSC-7 (Norwalk, CT). Samples were put into a lyophilizer for 1 h to remove the trace amount of solvents. Each sample (1.5–5.0 mg), weighed to the nearest 0.01 mg, was sealed in a stainless-steel pan. An empty pan was used as a reference sample. Heating and cooling rates were 5°C/min unless otherwise specified. The enthalpies of fusion (ΔH_m) and crystallization (ΔH_c) were determined by using 7 series/UNIX software. The machine was calibrated by using the data obtained from high purity standard material (indium). The estimated error margin for the indium standard is less than 0.5°C in the transition temperature and less than 2% in enthalpy. By systematically altering the thermal protocol, eight polymorphic phases were found.

These thermal protocols were developed to identify each of the phases.

α -Phase.² A solidified sample was melted at 35°C, and the isotropic liquid was cooled to 8°C. The α -phase so obtained is stable for ~4 h at 8°C.

β_4 -Phase. A crystalline sample was melted at 35°C, and the isotropic liquid was cooled to -1°C and incubated for 45 h at that temperature.

β_3 -Phase. A crystalline sample was melted at 35°C, and the isotropic liquid was cooled to 2°C and incubated for 6 h at that temperature.

β_2 -Phase. A crystalline sample was melted at 35°C, and the isotropic liquid was cooled to 8°C and incubated for 8 h at that temperature.

β_1 -Phase. A crystalline sample was melted at 30°C, and was held at that temperature for 1 h. The isotropic liquid was then cooled to -20°C.

β' -Phase. Slow evaporation of *sn*-SODG-hexane solution in a cold room at 4°C gave crystals of the β' phase.

γ_1 -Phase. A solidified sample was melted at 35°C, and cooled to the temperature between -3°C and -5°C.

γ_2 -Phase. A solidified sample was melted at 35°C, and cooled below -10°C.

Hydrated *sn*-SODG Samples containing water for DSC measurements were prepared by adding concentrated *sn*-SODG-hexane solution in the DSC pans, removing hexane by evaporation. The pans containing samples were maintained in a vacuum for 30 min. Samples were weighed and different amounts of water were added. The amount of water was estimated gravimetrically after the pans were sealed. Samples were heated to 35°C and shaken in pans for 15 min to equilibrate water with lipid. The samples

were checked for hydrolysis and 1,3-acyl migration by TLC (24). No hydrolysis or 1,3-acyl migration were detected. The amount of water bound to *sn*-SODG was determined by 1) measuring the ΔH of the water melting peak as a function of water/*sn*-SODG ratio; and 2) by analyzing the ^1H and ^{13}C spectra of the dry and hydrated *sn*-SODG. ^1H and ^{13}C spectra were obtained on a Varian 300 NMR spectrometer.

These thermal protocols were developed for the phases of *sn*-SODG with water (subscript w is used to differentiate from the dry phases).

β_w -Phase. Samples were melted at 35°C, then cooled to 8°C, and incubated at that temperature for 20 min.

α_w -Phase. Samples were melted at 35°C, then cooled to 8°C. The α_w phase so obtained is stable for less than 15 min.

γ_w -Phase. Samples were melted at 35°C then cooled to -20°C.

X-ray powder diffractions

X-ray powder diffraction patterns of each sample were recorded using nickel-filtered $\text{CuK}\alpha$ radiation from an Elliot GX-6 (Elliot Automation, Borehamwood, U.K.) rotating-mode generator equipped with cameras using Franks double-mirror optics (30) and toroidal-mirror optics. The samples were packed into 0.7- or 1.0-mm diameter Lindeman capillaries (Charles Supper, Natick, MA), sealed, and examined in variable-temperature sample holders. The rate of cooling and heating to a fixed temperature is 2–4°C/min. The photos were taken on a Toroid camera unless otherwise specified. The diffraction patterns were recorded using thermal programming similar to those used in the DSC investigation.

α -Phase. A melted sample was heated to 40°C for 30 min, and cooled to 8°C. X-ray diffractions were recorded for 4 h on a Franks camera.

β_4 -Phase. A sample crystallized from solvent was melted and heated to 40°C for 1 h (this temperature is 5°C higher than that used for the DSC protocol to avoid the crystallization of β_1 due to a somewhat greater temperature variation in the X-ray camera), then cooled to -1°C, and incubated at -1°C for 45 h. X-ray diffractions were recorded for 60 h on a Franks camera.

β_3 -Phase. A sample crystallized from solvent was heated to 40°C for 1 h, then cooled to 2°C, and incubated at 2°C for 10 h. X-ray diffractions were recorded for 24 h.

β_2 -Phase. A sample crystallized from solvent was heated to 40°C for 1 h, then cooled to 8°C, and incubated at 8°C for 8 h. X-ray diffractions were recorded for 24 h.

β_1 -Phase. A sample crystallized from solvent was heated to 30°C for 1 h, then cooled down to -20°C. X-ray diffractions were recorded for 24 h.

β' -Phase. Crystalline powder from hexane was transferred at 0°C to the camera. The X-ray diffractions were recorded at 15°C for 48 h on a Franks camera.

²The nomenclature of α , β , and β' phases is based on Larsson's classification (13, 25). The wide angle spacings which reflect chain packing show a single sharp reflection at 4.1–4.2 Å in the α phase; a strong reflection at ~4.6 Å and other reflections in the β phase and strong reflections at ~4.2 and 3.8 Å in the β' phase. The γ phase nomenclature is based on the nature of transformation for unsaturated fatty acid chains (26–29).

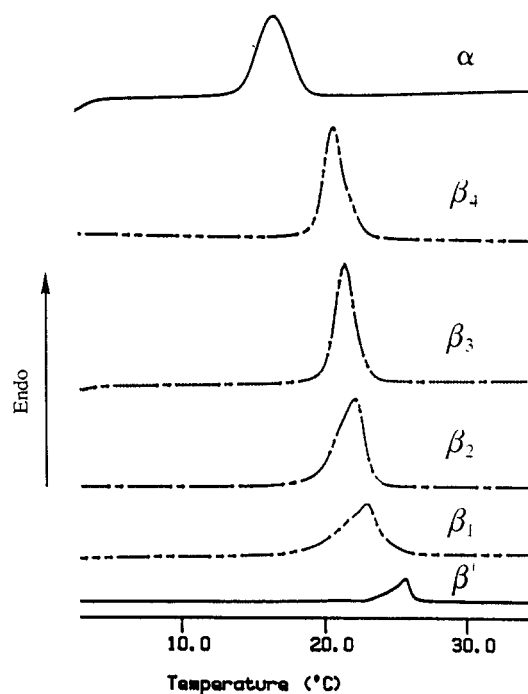


Fig. 1. DSC melting curves for six phases of *sn*-SODG (the area of the peaks does not correspond to ΔH_m). The β' -phase was heated at $1^\circ\text{C}/\text{min}$, the others were at $5^\circ\text{C}/\text{min}$. The thermodynamic data and X-ray diffractions are summarized in Table 1 and Table 2.

β_w -Phase. The sample was made with 30% water. Sample was melted at 35°C for 15 min, then cooled to 8°C , and incubated at that temperature for 1 h. X-ray diffractions were recorded at 8°C for 20 h on a Franks camera.

RESULTS

Dry *sn*-SODG

Dry *sn*-SODG sample revealed eight polymorphs and hydrated only three. The results on dry *sn*-SODG will be discussed first followed by results on hydrated samples. The DSC traces of simple heating and cooling process ($0.1^\circ\text{C}/\text{min}$) showed complicated crystallization and melting behavior characteristic of marked polymorphism. However, the isolation of each phase was achieved by changing the crystallization condition (heating patterns, incubation temperature, and time, crystallization from solvent). **Fig. 1** displays the melting peaks of six of the polymorphs for *sn*-SODG. The thermodynamic data of each polymorph are given in **Table 1**. The X-ray diffraction data are given in **Table 2**.

Fig. 2 (incubation time < 3 h) shows the formation of α -phase. The α -phase is obtained from a melted melt-crystallized sample. It is formed by cooling ($5^\circ\text{C}/\text{min}$) of the melt to 8°C . The sample is stable only for about 4 h

at 8°C . It will then transform to other phases (e.g., β_2 -phase). In fact, some small transformation of the α -phase to the β_2 -phase occurs as early as 3 h (**Fig. 2**). The α -phase obtained from solvent (hexane) crystallized sample can only be obtained by heating the isotropic liquid to higher than 32°C (lower than 32°C will give β_1 when cooled) and then cooling to 8°C . The α -phase obtained this way is less stable than those from melt-crystallized samples (see below). The melting point (T_m) of α -phase is 16.4°C ; the crystallization temperature (T_c), 12.5°C and the enthalpy of fusion (ΔH_m), 6.8 kcal/mol. X-ray diffractions show α -phase has a single intense wide-angle diffraction (**Fig. 3**), 4.25 Å is indicative of hexagonal chain packing. The α -phase has a calculated long spacing of 174 Å, which corresponds to eight asymmetric layers. The α -phase reversibly transforms to γ_1 -phase and then γ_2 -phase by cooling ($5^\circ\text{C}/\text{min}$), (see **Fig. 4a** and **b**): $T(\gamma_1)$; -2.9°C , $\Delta H(\gamma_1)$; 0.47 kcal/mol; $T(\gamma_2)$; -5.9°C , $\Delta H(\gamma_2)$; 1.18 kcal/mol. We were not able to obtain X-ray diffraction patterns for γ_1 and γ_2 , because these phases are unstable at low temperatures below which γ_1 and γ_2 formed and transformed to other phases (mixed β -phases) in a few minutes (see **Fig. 4b**).

The formation process of β_4 is shown in **Fig. 5**. Cooling of an isotropic liquid from 35°C gave the α -phase (see above). Incubation at -1°C for 45 h produces nearly pure β_4 -phase. Incubation at -1°C for less time produces a complicated process, melting of α -phase, crystallization of β_3 , and partial formation of β_4 . The β_4 -phase obtained after 45 h incubation at -1°C melts at 20.7°C ; ΔH_m , 13.8 kcal/mol. The wide-angle X-ray diffraction pattern

TABLE 1. Thermodynamic data of eight phases of dry *sn*-SODG and the three hydrated phases of *sn*-SODG

Phase	T_m^a	ΔH^b	ΔS^c	T_c^d
	$^\circ\text{C}$	kcal/mol	cal \cdot $K^{-1} \cdot$ mol $^{-1}$	$^\circ\text{C}$
Dry				
β'	25.7	11.9	39.8	
β_1	23.1	12.3	41.5	17.4
β_2	22.2	14.4	48.9	
β_3	21.5	13.8	47.0	
β_4	20.7	13.8	47.0	
α	16.4	6.80	23.5	12.5
γ_1	-2.9	0.47	1.72	-5.5
γ_2	-5.9	1.18	4.42	-10.9
Hydrated				
β_w	19.9	14.3	48.8	
α_w	15.1	6.9	23.2	11.9
γ_w	-12.0	0.79	3.03	^f

^aTemperature of melting transition peak value.

^bEnthalpy of melting.

^cEntropy of melting transition calculated from the enthalpy of melting transition.

^dTemperature of crystallization transition peak value.

^ePhysical data for polymorphic transformation not melting.

^fOverlap with water peaks.

TABLE 2. X-ray spacings (\AA) of six of the eight phases of dry *sn*-SODG and the β_w phase of hydrated *sn*-SODG^a

β'	β_1	β_2	β_3	β_4	α	β_w (Hydrated)
47.1 av.	34.5 av.	43.4 av.	44.7 av.	46.1 av.	174 av.	43.7 av.
47.1 (vs),1	34.4(vs),1	43.6(vs),1	44.6(vs),1	46.1(vs),1		43.5(vs),1
23.6 (w),2		21.6(s),2	22.3(s),2	23.1(m),2	86.0(w),2	21.9(vw),2
15.7 (s),3	11.5(s),3	14.5(vs),3	14.9(vs),3	15.3(s),3	58.0(m),3	14.6 (w),3
		11.0(m),4			43.5(s),4	
	6.90(m),5	8.63(m),5	8.94(m),5	9.20(w),5		
7.85(w),6		7.23(w),6	8.19(w)		29.0(m),6	
7.40(w)	4.92(w),7	6.18(w),7	5.28(w)			
6.96(w)						
6.49(w)						
5.99(w)						
5.50(w)					17.4(w),10	
5.14(w)						
4.81(w)						
4.69(w)	4.60(vs) ^c	4.61(vs) ^c	4.65(vs) ^c	4.72(vs) ^c		4.71(w) ^c
4.52(m)		broad		broad		broad
4.48(m)		4.41(vs) ^d	broad	4.58(s) ^d		4.36(w) ^d
4.34(s)	broad ^b		4.34(vs) ^d	4.40(s)		
4.31(w)						
4.23(m)						
4.09(vs)	4.01(vs) ^d	4.11(vs)	4.16(vs)	4.21(s)	4.25(s)	4.22(w)
3.92(w)	3.92(vs) ^c					
3.88(s)	broad	3.81(s)				
	3.61(vs) ^d	3.58(m)				
	3.21(m)					

^aAv., average 001 spacing calculated from all the orders. Relative intensity is given in parentheses: vs, very strong; s, strong; m, medium; w, weak. The order of 001 reflection is indicated after the diffraction long spacing intensity.

^{b,c,d}Reflections diffuse between c and d.

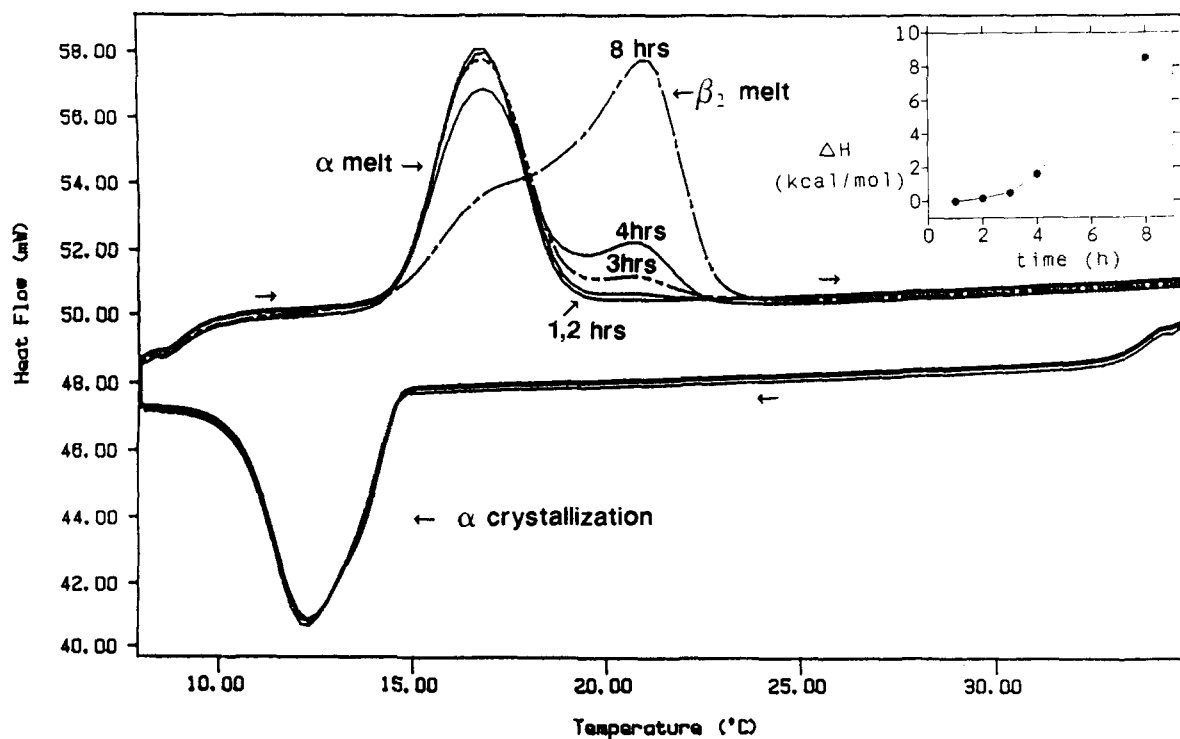


Fig. 2. Transformation of α -phase to β_2 -phase at 8°C as a function of incubation time. DSC curves are: cooling from 35°C to 8°C , incubation at 8°C for 1, 2, 3, 4 and 8 h, and then heating from 8°C to 35°C . Inset shows $\Delta H_m(\beta_2)$ versus incubation time. A very small amount of β_2 phase has formed by 3 h and by 8 h the transformation to β_2 phase is nearly complete.

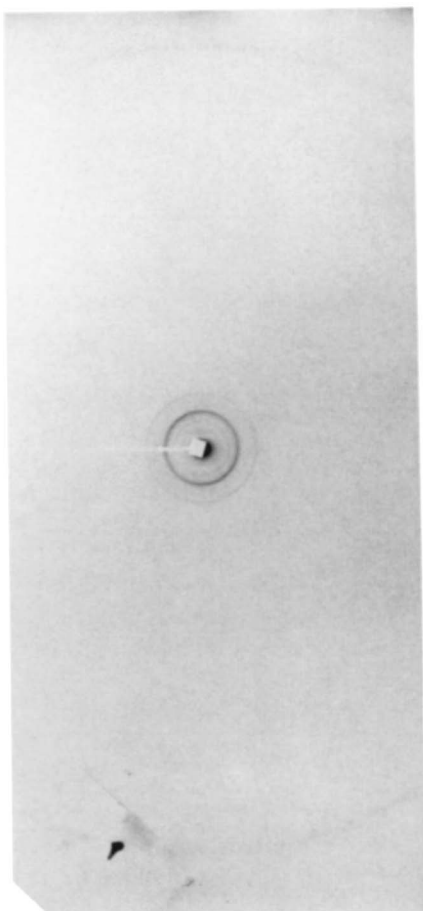


Fig. 3. X-ray Franks diffraction photo of the α -phase at 8°C, 4 h.

showed broad diffractions at 4.72–4.40 Å and 4.21 Å (Fig. 6). The long spacing is 46.1 Å.

The formation processes of β_3 and β_2 are similar to that of β_4 . Cooling of an isotropic liquid from 35°C gave the α -phase (see above). Incubation at 2°C for 6 h produces nearly pure β_3 -phase. The β_3 -phase melts at 21.5°C; ΔH_m , 13.8 kcal/mol. The X-ray pattern showed very broad and intense diffractions at 4.65–4.34 Å and 4.16 Å. This is an indication of a somewhat disordered β subcell (13, 25). The lamellar repeat is 44.7 Å.

Cooling of an isotropic liquid produced by melting hexane crystallized *sn*-SODG from 35°C gave the α -phase. Incubation at 8°C for 8 h produced mainly the β_2 -phase. β_2 melts at 22.2°C; ΔH_m , 14.4 kcal/mol. The X-ray pattern showed very broad and intense diffractions at 4.61–4.41 Å, and 4.11 Å. This indicates a somewhat disordered β subcell. The lamellar repeat is 43.4 Å.

The β_1 -phase is formed by melting a solvent (hexane) crystallized sample at 30°C for 1 h to remove the seeds of β' (higher than 32°C will give α -phase when cooling), and then cooling to below 17.4°C. Fig. 7 shows the formation of β_1 . T_m , 23.1°C; T_c , 17.4°C; ΔH_m , 12.3. X-ray pattern showed very broad and intense diffractions at 4.60–4.01 Å, and 3.92–3.61 Å. This is an indication of a somewhat disordered β subcell (13, 25). The lamellar repeat is 34.5 Å.

sn-SODG crystallized from hexane at 4°C by slow evaporation gave β' which melts at 25.7°C; ΔH_m , 11.9 kcal/mol (see Fig. 1). The X-ray small-angle pattern of β' has many fine structural features (Fig. 8). The wide-angle

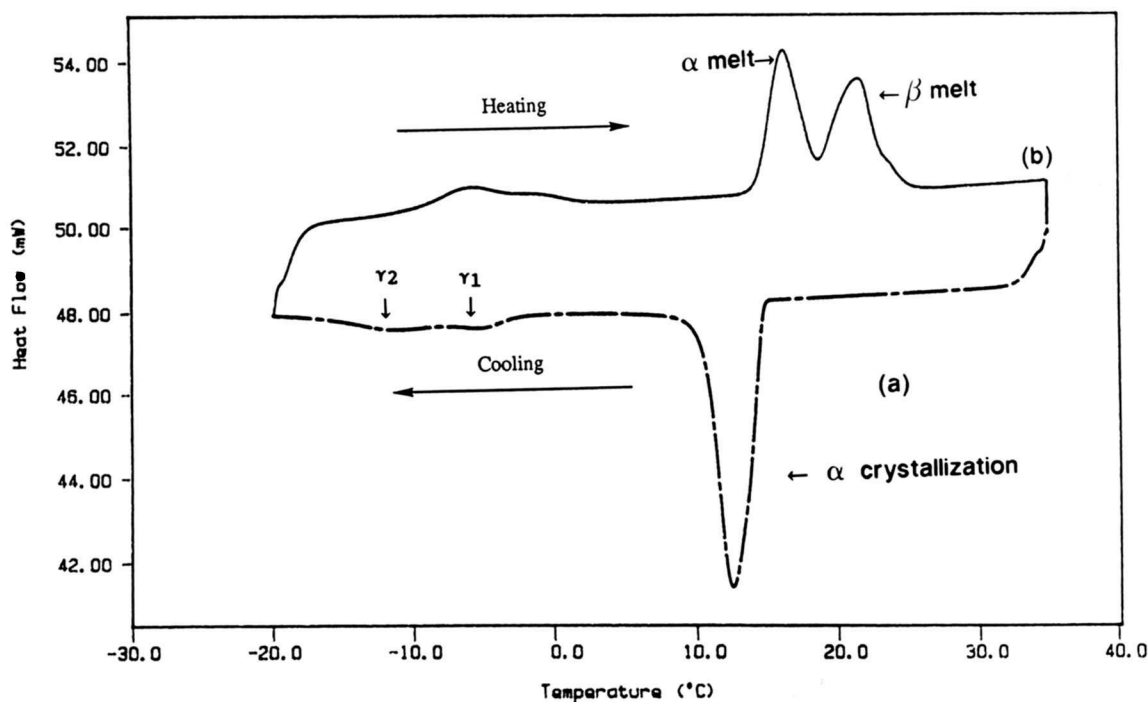


Fig. 4. Formation of γ_1 phase and γ_2 phase. (a) Cooling at 5°C/min from 35°C to -20°C first gives α -phase, which then transforms to γ_1 and then γ_2 . (b) Heating at 5°C/min from -20°C to 35°C transforms γ_2 to γ_1 and then partly to the α -phase. Some β phases were formed during temperature reversal at -20°C that melted above the α -phase.

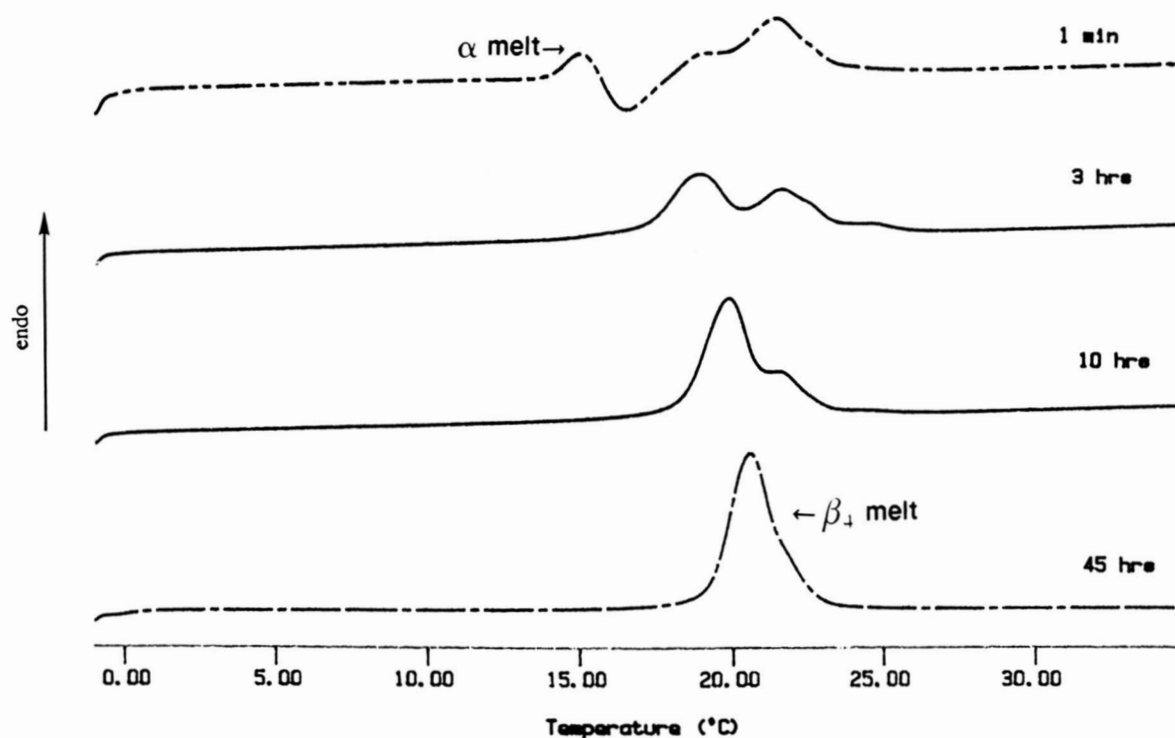


Fig. 5. Formation of the β_4 phase. The four heating curves ($5^\circ\text{C}/\text{min}$) are incubations at -1°C for 1 min, 3, 10, and 45 h after cooling from 35°C ($5^\circ\text{C}/\text{min}$).

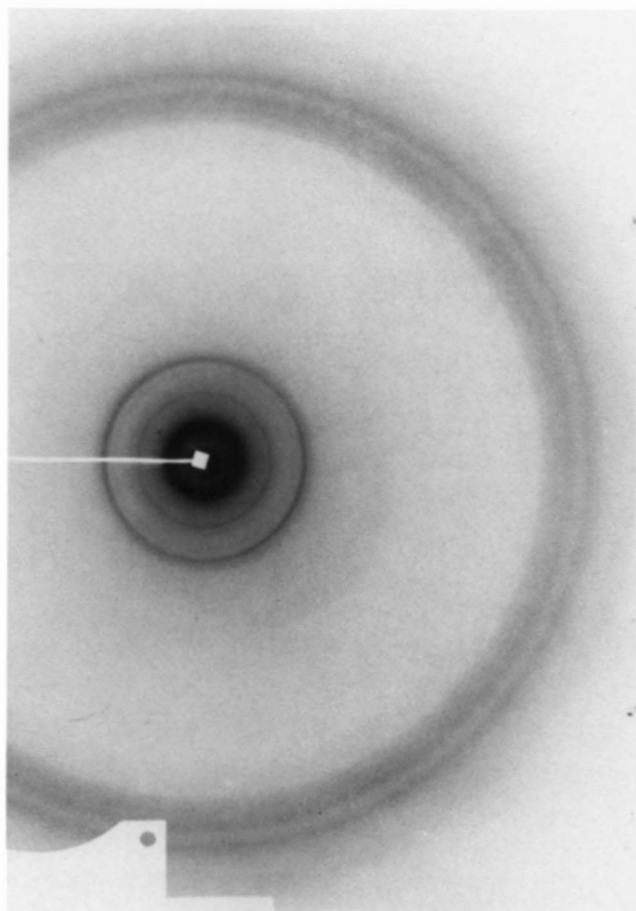


Fig. 6. X-ray Franks diffraction photo of the β_4 phase at -1°C , 60 h.

diffractions 4.38, 4.09, and 3.88 \AA indicated that it has a β' structure ($0 \perp$) (13, 25). The β' phase has a lamellar repeat of 47.1 \AA .

Hydrated *sn*-SODG

To determine the amount of water incorporated into *sn*-SODG, the water(mg)/*sn*-SODG(mg) ratio was plotted against ΔH_m of the H_2O melting. Eight values from weight ratios of 0.043 to 0.618 were studied. With 0.043 $\text{H}_2\text{O}/\text{sn}$ -SODG ratio, no H_2O melting was noted indicating that the water was bound. The line describing the relation was: $\text{water(mg)}/\text{sn-SODG(mg)} = 0.0120 \Delta H_m + 0.0187$. ΔH_m of water determined from the slope is 83.3 cal/g . The error is less than 5%, indicating reasonable accuracy. The intercept indicated 0.67 mol of $\text{H}_2\text{O}/\text{sn}$ -SODG but the standard deviation of the intercept was high and allowed from 0 to 1.3 mol $\text{H}_2\text{O}/\text{sn}$ -SODG. Therefore we used ^1H and ^{13}C NMR to trace the water effect on liquid *sn*-SODG.

Liquid *sn*-SODG was put in a capillary cylinder ($8 \mu\text{l}/\text{cm}$, Wilmad) and the contents were mixed with water (30% by volume) by centrifuge in the sealed capillary cylinder. After mixing, the capillary tube was placed in an ultracentrifuge and spun in an SW41 rotor for 30 min at 15,000 rpm to separate the two phases completely. The capillary cylinder with sample was then inserted in a 5-mm NMR tube containing CDCl_3/TMS . Comparison of ^1H NMR spectra between the neat liquid of *sn*-SODG and *sn*-SODG/water shows that there is an

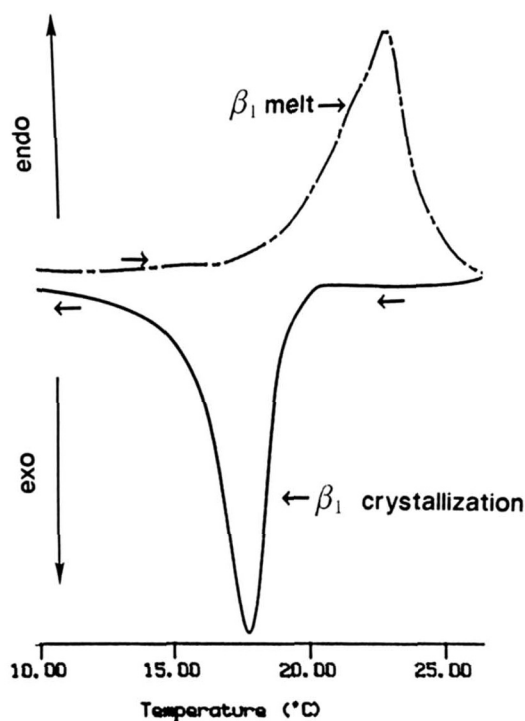


Fig. 7. Formation of the β_1 phase. Cooling from 30°C to -20°C at 5°C/min after incubation at 30°C for 1 h crystallized β_1 . Heating from -20°C at 5°C/min melts β_1 (only partial region is shown).

extra peak at 4.75 ppm (equivalent to 1 proton), which is different from that of the unbound water (4.82 ppm, in the blank experiment). Therefore, on a time average, each *sn*-SODG binds to half of an H₂O molecule. The -OH group of *sn*-SODG shifts from 4.31 to 4.11 ppm upon forming a water complex. The upfield shifts of both H₂O and -OH in the *sn*-SODG/water complex suggest that the H-bonding is weaker compared to pure water and pure liquid *sn*-SODG. ¹³C NMR shows that the 3 *sn*-glycerol carbon, -CH₂-OH, shifts upfield from 60.91 to 60.75 ppm while the *sn*-1 carbon, CH₂-OCO- shifts downfield from 62.72 to 62.85 when H₂O is added. Also, the two carbons of the C=O groups shift downfield by 0.2 ppm while the other carbons shift less than 0.04 ppm after adding water, consistent with the previous study on hydration of diglyceride carbonyls (11). Taken together, the ¹H and ¹³C NMR results indicate the formation of an *sn*-SODG/water complex with H₂O loosely H-bonding to the polar region of the diglyceride molecule.

Eight samples containing different amounts of water were used for the DSC measurement. Only three phases were detected for *sn*-SODG in all these samples, e.g., α_w , β_w , and γ_w phase. The α_w -phase has T_m, 15.1°C, ΔH_m , 6.70 kcal/mol. The β_w phase has T_m, 19.9°C, ΔH_m , 14.3 kcal/mol. The transition temperature from α_w to γ_w is -12.0°C, ΔH , 0.79 kcal/mol. The α_w phase is not stable. It transforms to β_w phase in less than 15 min. The melting point of the α_w phase is about 1°C lower than the α -

phase of the dry state, though ΔH_m is about the same (6.70 and 6.80 kcal/mol).

In the presence of water, the phase behavior of *sn*-SODG is simplified. X-ray diffractions of β_w are: 43.5(vs),1; 21.9(vw),2; 14.6(w),3; 4.71(w) broad 4.36(w); 4.22(w). The bilayer periodicity is the same as dry β_2 phase but the intensities are different indicating that β_w is not the same structure as β_2 or any other dry β phase.

DISCUSSION

Lamellar structure

The long spacings of the six phases of *sn*-SODG can be divided into three groups: 1) ~ 45 Å, β_4 (46.1), β_3 (44.7), β_2 (43.4), β' (47.1); 2) 35 Å, β_1 (34.5); (3) 174 Å, α (174). The first set of long spacings is similar to the length of bilayers of the known DG and TG containing stearyl and oleoyl chains (40-55 Å) (31, 32). Therefore, the four phases (β_4 , β_3 , β_2 and β') have bilayer structures. The intensity of the first three reflections in these four phases have $I(d_{001}) > I(d_{003}) > I(d_{002})$, which is also characteristic for a bilayer structure of fatty acids and mono-acid

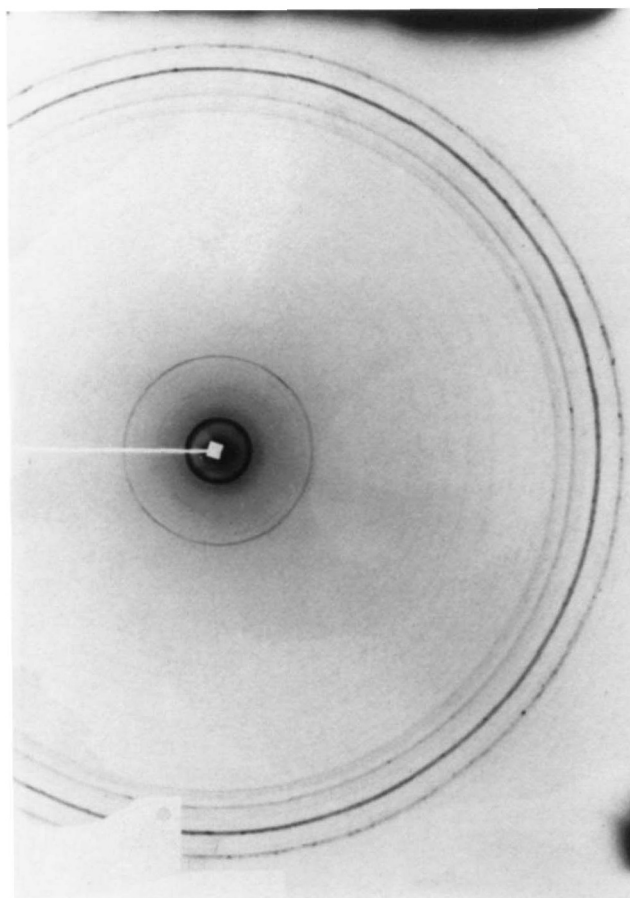


Fig. 8. X-ray Franks diffraction photo of the β' phase at 15°C, 48 h.

DGs and TGs (26). In the α -phase of *sn*-SS (10), SSS (33), OSO (21), and SOS (26), the molecular axes are suggested to be perpendicular to the base plane. Therefore, the average bilayer length of stearyl-oleoyl glycerols is 51 ± 3 Å. If we use this as the estimate bilayer length of *sn*-SODG, the tilt angles with respect to the base plane for different phases are: β_4 , 65° ; β_3 , 61° ; β_2 , 58° ; β' , 67° . Thus, these phases not only have very similar energies, but also similar lamellar structures. The β_1 phase has a lamellar spacing of 34.5 Å, which is shorter than the other four bilayered phases. The even reflections are absent in the β_1 phase. The molecular axis is tilted more towards the base plane (43°) in the bilayer structure. The lamellar repeat for the α -phase is most unusual (174 Å), a structure of eight asymmetric layers! The long range ordering of *sn*-SODG is higher than that of mixed chain triglycerols (six layers ~ 120 – 130 Å) (20, 21, 26).

Subcell structure

The α form of *sn*-SODG packed in a hexagonal array, giving a single very strong reflection at 4.25 Å. Hence, the stearyl and oleoyl chains in the diglycerol were arranged as rotationally disordered. The four β phases (β_1 , β_2 , β_3 , β_4) all have an intense reflection 4.60–4.72 Å,

characteristic of a β -type packing (13, 25). However, all these phases show broad diffraction rings in the short spacing region (Table 2, Fig. 6), suggesting that they have complicated and probably somewhat disordered chain arrangement. In contrast, the β' phase has many fine and sharp reflections. The three most intense short spacings are: 4.34(s), 4.09(vs), 3.88(s). Therefore, the molecules in this phase adopted an $O \perp$ packing arrangement (13, 25). Subcell structure of $O \perp$ for a *cis*-monounsaturated fatty acid was first found in petroselenic acid (low melting form) (34). This requires the molecular axis not to be perpendicular to the glide plane (**b**-glide). The molecular axis of β' is 67° to the base plane, which is reasonable for a $O \perp$ subcell.

Packing of *sn*-SODG chains

The β and β' phases of *sn*-SODG packed in a bilayer structure. However, from the long and short spacings one cannot determine whether the bilayer structure adopts a hairpin [like simple 1,2-*sn*-diglycerols (8–10)] or an extended linear or V-shape [like 1,3-diglyceride of 11-bromoundecanoic acid (19)] conformation. A molecular modeling study on 1,2-*sn*-SODG gave interesting results (15–17). The calculation proceeded by assuming 1) 1,2-*sn*-

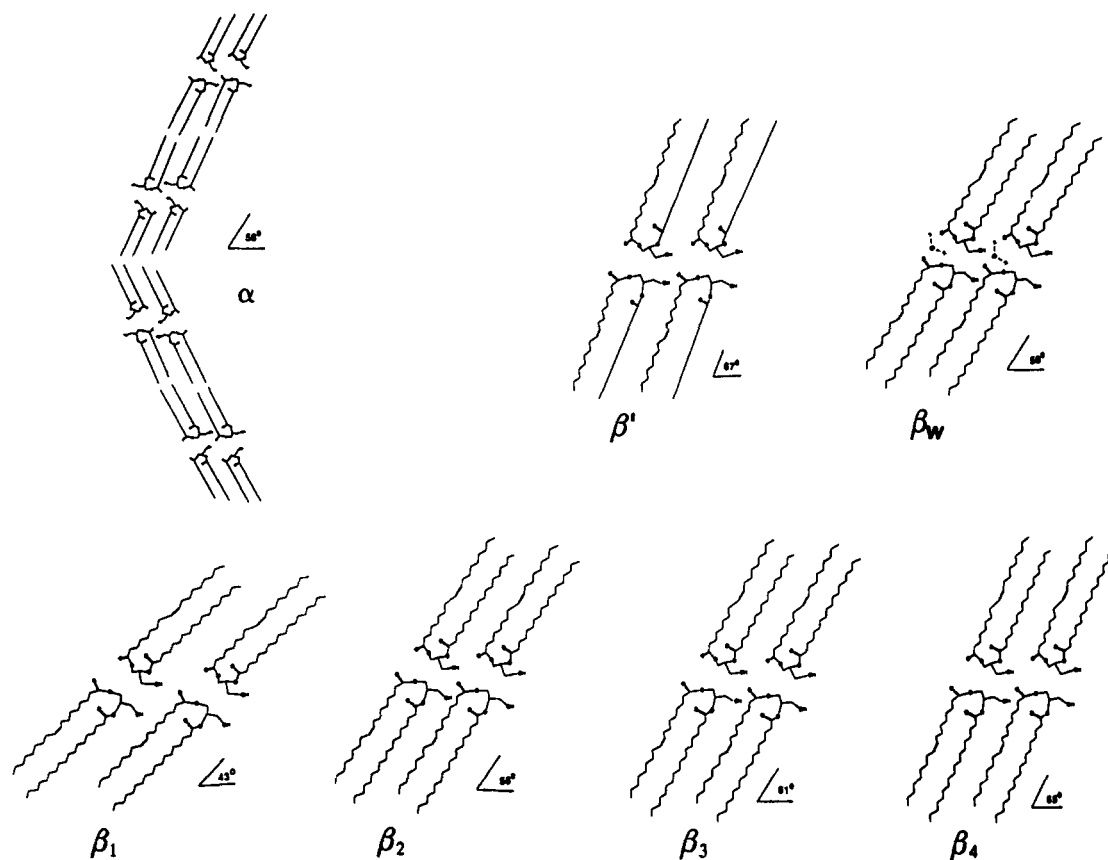


Fig. 9. Possible structures of *sn*-SODG. The headgroup conformations are assumed to be similar to 1,2-dilauroyl-*sn*-glycerol (8). The angles of tilt and chain conformations are based on X-ray long and short spacings. The conformation around the double bond is unknown.

SODG adapted hairpin conformation identical to the conformation of dilauroyl phosphatidylethanolamine (PE) determined by single crystal X-ray diffraction (18); 2) the oleoyl chain has a *trans-antiskew-cis-antiskew-antigauche-trans* torsion sequence about the double bond. This is very similar to the torsion sequence of the oleoyl group in the single crystal structures of cholesteryl oleate at 123°K (35). The results showed: a) the conformation of oleoyl was highly irregular in 1,2-*sn*-SODG. This irregularity was caused by the *cis* double bond. b) A single saturated chain helped to stabilize the conformation of the monoene and yield a lower packing energy. However, the monoene could not simultaneously achieve optimum contacts when placed between two saturated chains, and the packing energy per interacting pair of molecules was consequently higher. c) The molecule resisted being placed in the conformation which would create maximal van der Waals contacts between the straight *sn*-1 chain and the kinked *sn*-2 chain by tilting the mean axis of the latter.

These results seemed not to favor the hairpin conformation, although it had been imposed by the constraints adopted. However, as indicated by mixed chain triglycerols (21, 22, 26), stearyl and oleoyl chains certainly have the ability to pack together. If the oleoyl chain

adopted a different torsion sequence, the result might be surprising. X-ray single crystal studies of three molecules containing the oleoyl group showed that the methylene groups around the double bond are quite flexible and can adopt many torsion sequences. The torsion sequence around the double bond of oleic acid is *skew-cis-antiskew* (132°, -2°, -128°) (36) while that of cholesteryl oleate at 123°K (35) is *skew-cis-skew-gauche* (128°, 1°, 123°, 70°). Furthermore, even for the same compound, cholesteryl oleate, different temperatures gave different conformation of the oleoyl chains. The conformation of the oleoyl chain in cholesteryl oleate at 295°K (37) has many more *gauche* bonds than that at 123°K. Recent studies on the single crystal structures of *cis*-monounsaturated fatty acids provide further information about the torsion preferences around the double bond. The γ_1 phase of erucic acid (38) has *skew-cis-skew* (98°, 2°, 95°) torsion sequence; the low melting phase of petroselinic acid (34) has *skew-cis-antiskew* (157°, 0°, -160°); the high melting phase (39) has two independent molecules: 1) *skew-cis-skew* (91°, 1°, 130°); *skew-cis-skew* (137°, 1°, 119°). This structural information indicates the torsion angles next to the *cis* double bond prefer to have *skew* or *antiskew* conformation. However, the degrees of the angles, the directions of the bend-

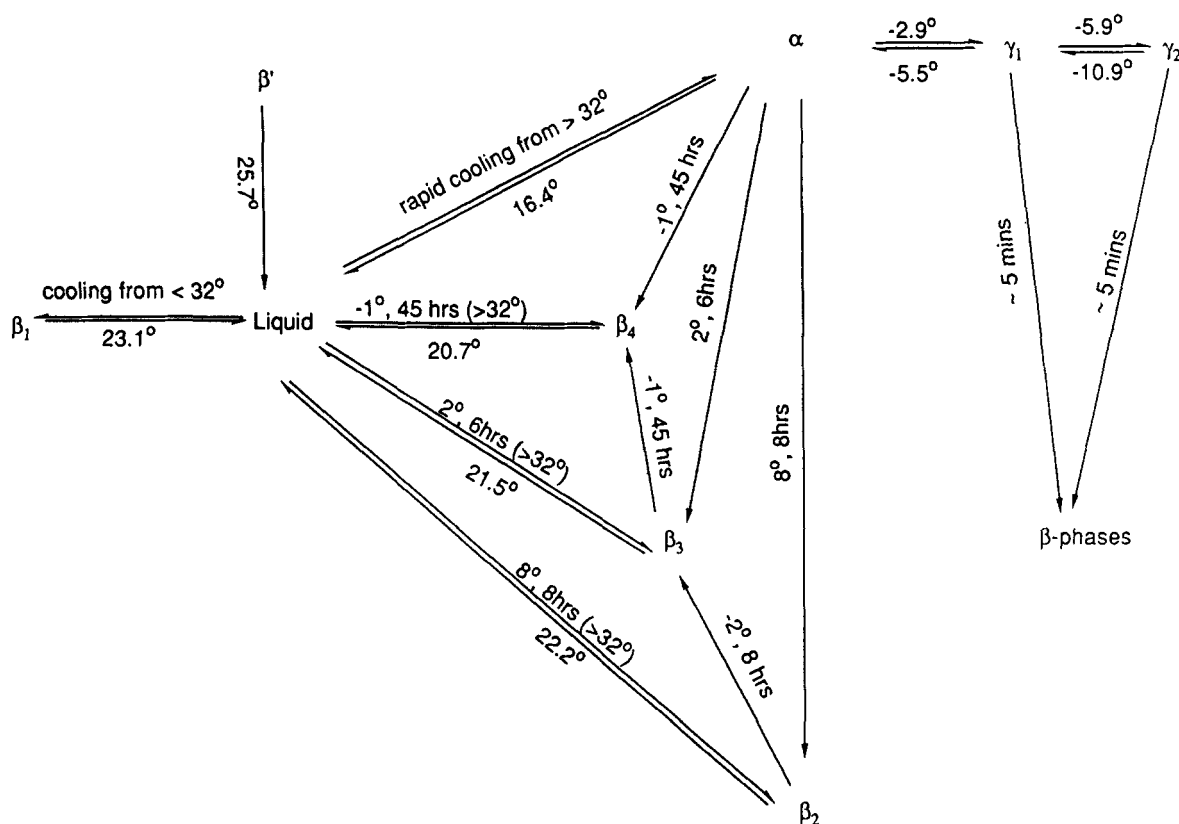


Fig. 10. Phase transformations of dry *sn*-SODG.

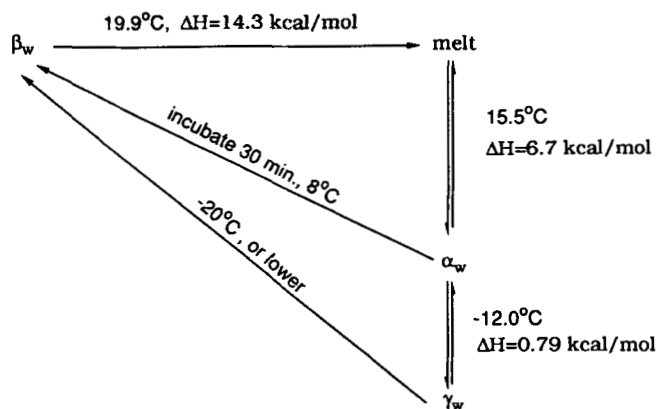


Fig. 11. Phase transformations of hydrated *sn*-SODG.

ing, and the rest of the torsion sequence are uncertain factors that can be changed to satisfy the structure and energy requirement.

Not only does the oleoyl chain have many flexibilities, but the stearoyl chain can also adapt *gauche* conformations along certain bonds. In the B-phase of stearic acid, the torsion angles of C1-C3 are in *gauche* conformation (40). Furthermore, the torsion angle around the carbons 2 and 3 of the *sn*-2 chain of phospholipids (41) and 1,2 dipalmitoyl 3-acetyl-*sn*-glycerol (42) is *gauche*. The structure differences and the conformational flexibilities

of the stearoyl and oleoyl chains probably provide the internal basis for the complex phase behavior of *sn*-SODG. The β and β' phases having very similar enthalpy and entropy of melting ($\Delta H \sim 13$ kcal/mol; $\Delta S \sim 44$ cal K⁻¹ mol⁻¹) are much less than saturated β' 1,2-DGs (1,2-SS, $\Delta H \sim 31$ kcal/mol; $\Delta S \sim 90$ cal K⁻¹ mol⁻¹). This suggests that *sn*-SODG phases take considerable energy to pack. The structure irregularity between stearoyl-oleoyl causes *sn*-SODG difficulties in finding a comfortable low energy arrangement.

The experiments with H₂O show each *sn*-SODG binds half a water molecule. This suggests that the molecules in this phase (β_w) have a hairpin conformation, with the hydrophilic heads (OH or C=O) H-bond to the H₂O molecules. We do not know the conformation around the glycerol of the dry phases. However, to go from an extended conformation with the two acyl chains pointing in opposite directions to a hairpin conformation with the chains lying side by side would entail marked changes that could only occur with partial melting. Since β_2 can transform to β_3 and β_4 without melting, it may also be a hairpin conformation. Also, α can transform to β_2 without melting. Thus we speculate that β_w , α_w , α , β_2 , β_3 , and β_4 all have hairpin conformations. Since the β' diffraction of *sn*-SODG is very similar to the β' -phase of 1,2-SS (10), the β' -phase of *sn*-SODG may also be in a hairpin conformation. Our best guess at the structure of the different

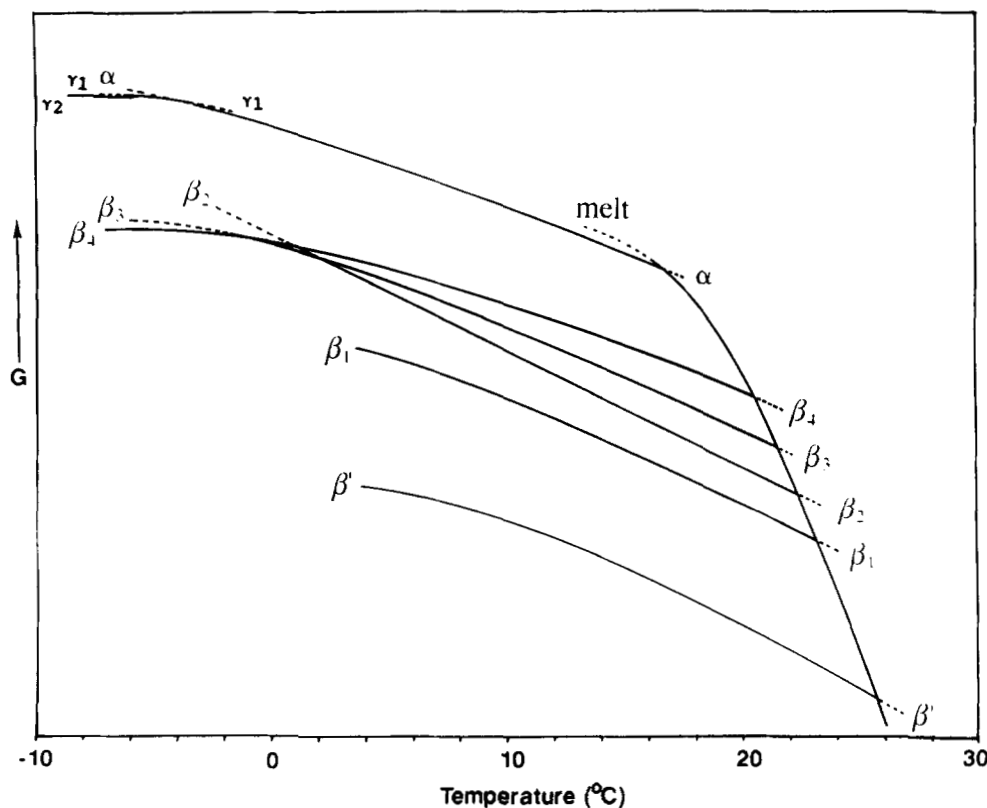



Fig. 12. Energy diagram for dry *sn*-SODG.

phases of *sn*-SODG is given in **Fig. 9**. The contribution of the double bond to the packing is probably to cause short range, local distortions of chain arrangements. Though the double bond does not fit well with the packing environment, it probably does not change the packing drastically from hairpin to an extended conformation.

The γ forms (γ_1 and γ_2) were only found on cooling of α -phases, the other β and β' phases did not have γ transformations when cooled to low temperature. The transition enthalpies for the γ phases are quite small (~ 1 kcal/mol). When the α -phase of saturated long-chain 1,2-DAGs is cooled they undergo a low enthalpy transformation to the "sub α -phase." This phase has a distorted hexagonal chain packing, something intermediate between a true hexagonal packing and orthorhombic perpendicular ($O \perp$) packing (10). It is possible that the γ forms described here represent such a structure. Transformations called γ were observed for unsaturated fatty acids with odd C atoms on the $-\text{CH}_3$ end [oleic acid (28) and erucic acid (29)]. These transformations are believed to be conformation changes from disorder to order (43). The disordered structures were caused by the rotational disorder of the methylene groups around the double bonds. It is well known that the metastable α -phase commonly has more disordered conformers than the stable phases (13).

Phase transformations and thermodynamic stability

The transformations between the eight phases of dry *sn*-SODG are complicated. **Fig. 10** shows the relationship between these phases. **Fig. 11** shows the relationship of the hydrated phases. The β' -phase crystallized from hexane melts to an isotropic liquid at 25.7°C. Cooling of the melted liquid will not give β' back. When the liquid was heated below 32°C, it crystallized β_1 . However, when the liquid was heated to above 32°C, it crystallized α and then transformed to other β phases according to different conditions. It appears that the liquid has a memory of certain structures. The relative thermodynamic stability for these phases is shown in the energy diagram (**Fig. 12**). Because the polymorphic transformation went monotropically, the order of stability is β' , β_1 , β_2 , β_3 , β_4 , and α . Because β_2 transforms to β_3 at 2°C, β_3 is more stable than β_2 below 2°C; β_3 transforms to β_4 at -1°C ; β_3 is less stable than β_4 below -1°C . Since α transforms to γ_1 and γ_2 reversibly, γ_2 is the most stable form at the temperature below -5.9°C among the three; γ_1 is the most stable form between -5.9°C to -2.9°C ; α is the most stable phase at higher than -2.9°C among the three. 

We wish to thank Dr. F. Kaneko of Osaka University for sending us the crystallographic data on petroselinic and erucic acids. We thank John Steiner and John Owusu-Djamboe for technical assistance, and Drs. Dharma Kodali and Rick Duclos for synthesizing the *sn*-SODG. We also thank Margaret Gibbons and Irene Miller for typing the manuscript. This work was sup-

ported by National Institutes of Health grants HL-26335 and HL-07291 (D. M. Small, P. I.).

Manuscript received 12 April 1993.

REFERENCES

- Small, D. M., and R. A. Zoeller. 1991. Lipids. In *Encyclopedia of Human Biology*. Vol. 4. Academic Press, New York. 725-748.
- Small, D. M. 1991. The effects of glyceride structure on absorption and metabolism. *Annu. Rev. Nutr.* **11**: 413-434.
- Berridge, M. J., and R. F. Irvine. 1984. Inositol triphosphate, a novel second messenger in cellular signal transduction. *Nature*. **312**: 315-321.
- Nishizuka, Y. 1984. The role of protein kinase C in cell surface signal transduction and tumor promotion. *Nature*. **308**: 693-698.
- Sekar, M. C., and L. E. Hokin. 1986. The role of phosphoinositides in signal transduction. *J. Membr. Biol.* **89**: 193-210.
- Rando, R. R., and N. Young. 1984. The stereospecific activation of protein kinase C. *Biochem. Biophys. Res. Commun.* **122**: 818-823.
- Ganong, B. R., C. R. Loomis, Y. A. Hannun, and R. M. Bell. 1986. Specificity and mechanism of protein kinase C activation by *sn*-1,2-diacylglycerols. *Proc. Natl. Acad. Sci. USA*. **83**: 1184-1188.
- Pascher, I., S. Sundell, and H. Hauser. 1981. Glycerol conformation and molecular packing of membrane lipids. The crystal structure of 2,3-dilauroyl-D-glycerol. *J. Mol. Biol.* **153**: 791-806.
- Dorset, D. L., and W. A. Pangborn. 1988. Polymorphic forms of 1,2-dipalmitoyl-*sn*-glycerol: a combined X-ray and electron diffraction study. *Chem. Phys. Lipids*. **48**: 19-28.
- Kodali, D. R., D. A. Fahey, and D. M. Small. 1990. Structure and polymorphism of saturated monoacid 1,2-diacyl-*sn*-glycerols. *Biochemistry*. **29**: 10771-10779.
- Hamilton, J. A., S. P. Bhamidipati, D. R. Kodali, and D. M. Small. 1991. The interfacial conformation and transbilayer movement of diacylglycerols in phospholipid bilayers. *J. Biol. Chem.* **266**: 1177-1186.
- Pearson, R. H., and I. Pascher. 1979. The molecular structure of lecithin dihydrate. *Nature*. **281**: 449-501.
- Small, D. M. 1986. The Physical Chemistry of Lipids from Alkanes to Phospholipids. *Handbook of Lipid Research Series*. Vol. 4. D. Hanahan, editor. Plenum Press, New York. 1-672.
- Small, D. M. 1984. Lateral chain packing in lipids and membranes. *J. Lipid Res.* **25**: 1490-1500.
- Applegate, K. R., and J. A. Glomset. 1986. Computer-based modeling of the conformation and packing properties of docosahexaenoic acid. *J. Lipid Res.* **27**: 658-680.
- Applegate, K. R., and J. A. Glomset. 1991. Effect of acyl chain unsaturation on the conformation of model diacylglycerols: a computer modeling study. *J. Lipid Res.* **32**: 1635-1644.
- Applegate, K. R., and J. A. Glomset. 1991. Effect of acyl chain unsaturation on the packing of model diacylglycerols in simulated monolayers. *J. Lipid Res.* **32**: 1645-1655.
- Hitchcock, P. B., R. Mason, K. M. Thomas, and G. G. Shipley. 1974. Structure chemistry of 1,2-dilauroyl-DL-phosphatidylethanolamine: molecular conformation and intermolecular packing of phospholipids. *Proc. Natl. Acad. Sci. USA*. **71**: 3036-3040.
- Hybl, A., and D. Dorset. 1971. The crystal structure of the

- 1,3-diglyceride of 11-bromoundecanoic acid. *Acta Crystallogr.* **B27**: 977.
20. Fahey, D. A., D. M. Small, D. R. Kodali, D. Atkinson, and T. G. Redgrave. 1985. Structure and polymorphism of 1,2-dioleoyl-3-acyl-*sn*-glycerols. Three- and six-layered structures. *Biochemistry*. **24**: 3757-3764.
21. Kodali, D. R., D. Atkinson, T. G. Redgrave, and D. M. Small. 1987. Structure and polymorphism of 18-carbon fatty acid acyl triacylglycerols: effect of unsaturation and substitution in the 2-position. *J. Lipid Res.* **28**: 403-413.
22. Kodali, D. R., D. Atkinson, and D. M. Small. 1989. Molecular packing in triacyl-*sn*-glycerols: influences of acyl chain length and unsaturation. *J. Dispersion Sci. Technol.* **10**: 393-440.
23. Kodali, D. R., and R. I. Duclos, Jr. 1992. Debenzylation and detritylation by bromodimethylborane: synthesis of mono-acid or mixed-acid 1,2- or 2,3-diacyl-*sn*-glycerols. *Chem. Phys. Lipids*. **61**: 169-173.
24. Kodali, D. R., A. Tercyak, D. A. Fahey, and D. M. Small. 1990. Acyl migration in 1,2-dipalmitoyl-*sn*-glycerol. *Chem. Phys. Lipids*. **52**: 163-170.
25. Larsson, K. 1966. Classification of glyceride crystal forms. *Acta Chem. Scand.* **22**: 2255-2260.
26. Sato, K., T. Arishima, Z. H. Wang, K. Ojima, N. Sagi, and H. Mori. 1989. Polymorphism of POP and SOS. I. Occurrence and polymorphic transformation. *J. Am. Oil Chem. Soc.* **66**: 664-674.
27. Sato, K., and M. Suzuki. 1986. Solvent crystallization of α , β and γ polymorphs of oleic acid. *J. Am. Oil Chem. Soc.* **63**: 1356-1359.
28. Suzuki, M., T. Ogaki, and K. Sato. 1985. Crystallization and transformation mechanisms of α -, β -, and γ -polymorphs of ultra-pure oleic acid. *J. Am. Oil Chem. Soc.* **62**: 1600-1604.
29. Suzuki, M., K. Sato, N. Yoshimoto, S. Tanaka, and M. Kobayashi. 1988. Polymorphic behavior of erucic acid. *J. Am. Oil Chem. Soc.* **65**: 1942-1947.
30. Franks, A. 1958. Some developments and application of microfocus X-ray diffraction techniques. *Br. J. Appl. Physics*. **9**: 349-352.
31. Ferguson, R. H., and E. S. Lutton. 1947. The polymorphism of triolein. *J. Am. Chem. Soc.* **69**: 1445-1448.
32. Daubert, B. F., and E. S. Lutton. 1947. X-ray diffraction analysis of synthetic unsaturated monoacid diglycerides. *J. Am. Chem. Soc.* **69**: 1449-1451.
33. Lutton, E. S., and A. J. Fehl. 1969. The polymorphism of odd and even saturated single acid triglycerols, C8-C22. *Lipids*. **5**: 90-99.
34. Kaneko, F., M. Kobayashi, Y. Kitagawa, Y. Matsuura, K. Sato, and M. Suzuki. 1992. Structure of the low-melting phase of petroselinic acid. *Acta Crystallogr.* **C48**: 1057-1060.
35. Gao, Q., and B. M. Craven. 1986. Conformation of the oleate chains in crystals of cholesteryl oleate at 123K. *J. Lipid Res.* **27**: 1214-1221.
36. Abrahamsson, S., and I. Ryderstedt-Nahringbauer. 1962. The crystal structure of the low melting form of oleic acid. *Acta Crystallogr.* **15**: 1261-1268.
37. Craven, B. M., and N. G. Guerina. 1979. The crystal structure of cholesteryl oleate. *Chem. Phys. Lipids*. **24**: 91-98.
38. Kaneko, F., M. Kobayashi, Y. Kitagawa, Y. Matsuura, K. Sato, and M. Suzuki. 1992. Structure of the γ_1 phase of erucic acid. *Acta Crystallogr.* **C48**: 1060-1063.
39. Kaneko, F., M. Kobayashi, Y. Kitagawa, Y. Matsuura, K. Sato, and M. Suzuki. 1992. Structure of the high-melting phase of petroselinic acid. *Acta Crystallogr.* **C48**: 1054-1057.
40. Goto, M., and E. Asada. 1978. The crystal structure of the B form of stearic acid. *Bull. Chem. Soc. Japan*. **51**: 2456-2459.
41. Hauser, H., I. Pascher, R. H. Pearson, and S. Sundell. 1981. Conformation of phospholipids. Crystal structure of a lysophosphatidylcholine analogue. *Biochim. Biophys. Acta*. **650**: 21-51.
42. Goto, M., D. Kodali, D. M. Small, K. Honda, K. Kozowa, and T. Uchida. 1992. Single crystal structure of a mixed chain triacylglycerol: 1,2-dipalmitoyl-3-acetyl-*sn*-glycerol. *Proc. Natl. Acad. Sci. USA*. **89**: 8083-8086.
43. Kobayashi, M., F. Kaneko, K. Sato, and M. Suzuki. 1986. Vibrational spectroscopic study on polymorphism and order-disorder phase transition in oleic acid. *J. Phys. Chem.* **90**: 6371-6378.